

Infrared and Fluorescence Assessment of the Hydration Status of the Tryptophan Gate in Influenza A M2 Proton Channel

Beatrice N. Markiewicz,¹ Thomas Lemmin,⁴ Wenkai Zhang,² Ismail A. Ahmed,³ Hyunil Jo,⁴

Giacomo Fiorin,⁵ Thomas Troxler,^{1,2} William F. DeGrado,^{4,} and Feng Gai^{1,2,*}*

¹Department of Chemistry, ²Ultrafast Optical Processes Laboratory, and ³Department of Biochemistry and Biophysics, University of Pennsylvania, Philadelphia, Pennsylvania 19104, United States

⁴Department of Pharmaceutical Chemistry, University of California San Francisco, San Francisco, California 94143, United States

⁵Institute for Computational Molecular Science, Temple University, Philadelphia, Pennsylvania 19122, United States

Supporting Information

Proton Flux Assay

A detailed description of the liposome flux assay can be found elsewhere.^{1,2} Briefly, the LUVs used in the proton flux measurements were prepared using a similar procedure described in the experimental section of the main text. Specifically, a peptide-lipid film composed of 25 nmol peptide (M2TM or M2TM-W_{CN}) and 25 μ mol lipid (the same as above) was rehydrated with 995 μ L of pH 7.4 potassium phosphate buffer (15 mM K_xPO₄ and 50 mM K₂SO₄). Immediately upon rehydration, 5 μ L of a pH indicator dye, pyranine (100 mM), was added to the mixture followed by freeze-thaw cycles and extrusion. The pyranine dye on the outside of the liposomes was removed by allowing this LUV solution to pass through a PD-10 column (GE Healthcare Life Sciences). To initiate the proton flux assay, 20 μ L of the newly prepared LUV solution was added to 2.5 mL of another buffer, that contains pH 7.4 sodium phosphate buffer (15 mM Na_xPO₄, 50 mM Na₂SO₄), 37.5 μ L of *p*-xylene-bis-pyridinium bromide (DPX) (1 M), which is a quencher of pyranine fluorescence, and 4 μ L of valinomycin (18 μ M). For measurements where the bulk (e.g. external buffer) was set to low pH, the sodium phosphate buffer was adjusted to pH 5.0 using 0.5 M H₂SO₄. The fluorescence kinetic traces were collected on a Cary Eclipse Fluorescence Spectrophotometer under constant stirring, using a time window of 100 s and a

time step of 0.25 s. The deprotonated pyranine fluorescence was excited at 460 nm and monitored at 515 nm, using a spectral width of 5 nm. At the end of each trial, the pyranine fluorescence intensity at 515 nm was collected again (integrated for 20 s) by exciting its pH-independent absorption isosbestic point at 417 nm. Dividing the fluorescence kinetics obtained with 460 nm excitation by this fluorescence signal helps remove any effects arising from differences in the sample concentrations and excitation intensities. Three trials were conducted and then averaged, yielding the reported kinetics.

The normalized fluorescence signal was further converted to intraliposomal proton concentration, $[H^+]$, using a calibration curve (Figure S1, ESI) determined by measuring the fluorescence of free pyranine dye in a series of potassium phosphate buffers with known pH values. Furthermore, the size and concentration of the LUVs, which were needed to determine the total intraliposomal volume, were measured using a fluorescence correlation spectroscopic setup described in detail elsewhere.³ Additionally, since the M2TM channel can orient with its N-terminus pointing toward either the interior ($N_{in}C_{out}$) or exterior ($N_{out}C_{in}$) of the liposome, we assumed there was a 1:1 ratio of these two orientations where only the $N_{out}C_{in}$ orientation is proton conducting, and as a result, divided the totally number of tetramers by a factor of 2.

Trp41 Rotamer Analysis

The Trp41 rotamer analysis using the $C\equiv N$ orientation angle of Trp_{CN} as a constraint was similar to that used by Hong and coworkers.⁴ First, four backbone structures, two for each pH condition (i.e., low and high), were chosen from the available M2TM structures in the Protein Data Bank (PDB) based on the similarity of their helix tilt angles to the experimentally determined values. Specifically, 3LBW and 2KQT were chosen for the high pH condition, and 2KAD and 3C9J were chosen for the low pH condition. Second, for each backbone structure, the Trp41 dihedral angles (χ_1 and χ_2) were systematically varied in a 1° increment using the VMD program,⁵ and for each (χ_1 and χ_2) combination the hypothetical $C\equiv N$ orientation angle was determined with respect to the z-axis of the channel. Third, for each case the RMSD value between the experimentally determined and the simulated $C\equiv N$ angles was calculated. Finally, plotting the dependence of the RMSD values on χ_1 and χ_2 yielded the 2D contour plot presented in the text. Out of the possible 7 rotamers that a Trp sidechain can sample, we rejected those that have a low RMSD value but encounter steric clashes with either the helix backbone or His37 residues.

Molecular Dynamics Simulations

To simulate M2TM- W_{CN} , the crystal structure of M2TM (PDB code 3LBW) was inserted in a $80 \times 80 \text{ \AA}^2$ 1-palmitoyl-2-oleoyl-*sn*-glycero-3-phosphocholine (POPC) patch. Each tryptophan was mutated to 5-cyanotryptophan (Trp_{CN}). Four different protonation states for the His37 were considered: His¹⁺, His²⁺, His³⁺, and His⁴⁺. The systems were solvated in a $80 \times 80 \times 100 \text{ \AA}^3$ water

box, neutralized through the addition of NaCl at a concentration of 150 mM. For comparison with the wild-type M2TM, we utilized the simulations conducted by Acharya *et al.*⁶

All simulations were performed using the NAMD 2.10 engine,⁷ with the CHARMM36 force field, including CMAP corrections for the protein and the POPC membrane.⁸ The parameters for Trp_{CN} were extracted from the 5-cyanoindole provided by the CHARMM general force field c36. TIP3P water parameterization was used to describe the water molecules.⁹ The periodic electrostatic interactions were computed using the particle-mesh Ewald (PME) summation with a grid spacing smaller than 1 Å. The systems were first equilibrated for 20 ns at 310 K with restraints on the backbone atoms. Free molecular dynamics were then performed up to 120 ns with a 2 fs integration time step using the RATTLE algorithm applied to all bonds. Constant temperature (310 K) was imposed by using Langevin dynamics,¹⁰ with damping coefficient of 1.0 ps. Constant pressure of 1 atm was maintained with a Langevin piston dynamics,¹¹ 200 fs decay period and 50 fs time constant.

Table S1: Dihedral angles of Trp_{CN}, $(\chi_1, \chi_2)_{\text{CN}}$, determined from the rotamer analysis using the dichroic ratio of the C≡N band. Also listed are the dihedral angles of Trp41, $(\chi_1, \chi_2)_{\text{PDB}}$, determined from the corresponding PDB structure.

pH	Backbone Structure	$(\chi_1, \chi_2)_{\text{PDB}}$	$(\chi_1, \chi_2)_{\text{CN}}$
Low	3C9J	(185°, 84°)	(162°, 93°) (185°, 62°)
	2KAD	(184°, 85°)	(165°, 105°)
High	3LBW	(178°, 79°)	(190°, 70°) (162°, 93°)
	2KQT	(185°, 78°)	(186°, 62°)

Table S2: Percentage of MD frames wherein the N-H group of Trp_{CN}41 or Trp41 is H-bonded to channel water within the time window of the MD simulation. Measurements were performed for each helix monomer in the channel. The wild-type M2TM data were determined from the simulations of Acharya *et al.*⁶

Protonation State	M2TM-W _{CN}	M2TM
His ⁺¹	28.35 ± 2.25 %	22.48 ± 2.16 %
His ⁺²	24.32 ± 4.61 %	23.48 ± 3.33 %
His ⁺³	14.82 ± 7.73 %	21.51 ± 2.24 %
His ⁺⁴	16.00 ± 6.18 %	20.28 ± 2.61 %

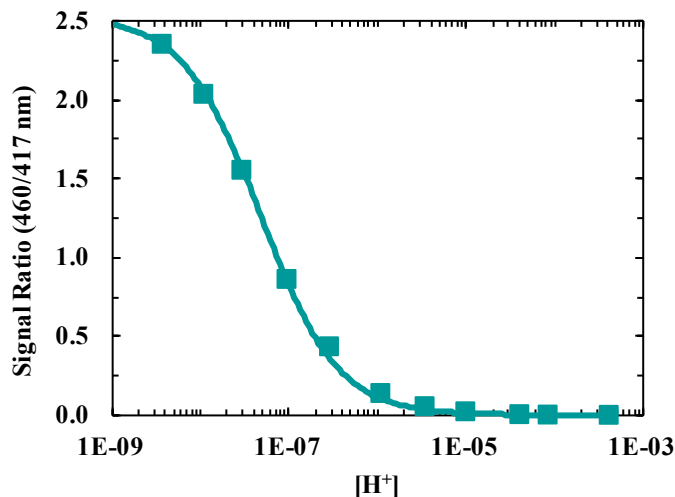


Figure S1: Pyranine fluorescence-pH calibration curve. The signal ratio is defined as the ratio between the fluorescence intensities obtained with excitation wavelengths of 460 nm and 417 nm, respectively. The smooth line is a fit of the data to the following equation: $S([H^+]) = A/(1+[H^+]/B)$, where $A = 2.53 \pm 0.02$ and $B = 4.79 \pm 0.18 \times 10^{-8}$ M.

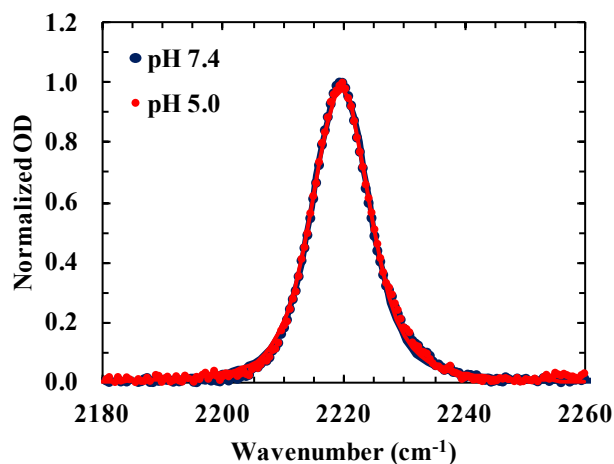


Figure S2: Comparison of the C≡N stretching vibrational bands of M2TM- W_{CN} in DPC micelles at pH 5.0 and 7.4. The smooth lines are fits to a Voigt profile.

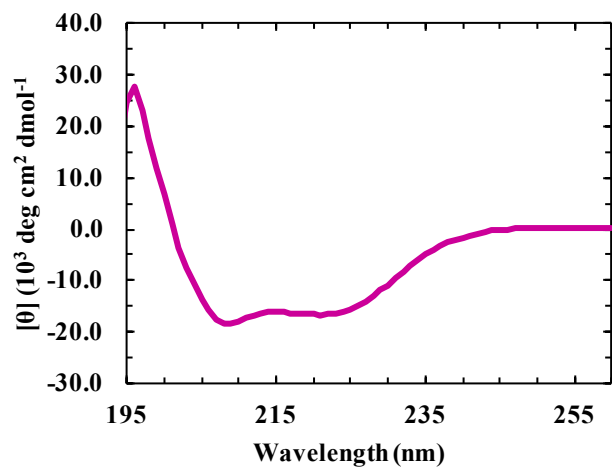


Figure S3: CD spectrum of wild-type M2TM in DPC micelles (1:35 peptide to lipid ratio) at pH 7.4. The final peptide concentration was approximately 50 μM .

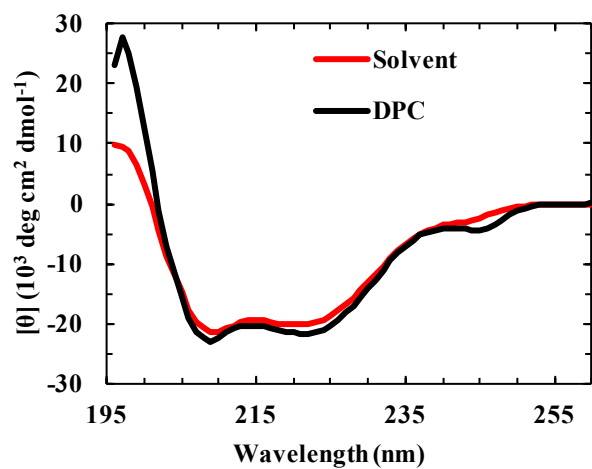


Figure S4: CD spectra of M2TM- W_{CN} in DPC micelles (1:35 peptide to lipid ratio) at pH 7.4 and in a solvent consisting of 2-propanol and H_2O (40:60), as indicated. The final peptide concentration was approximately 70 μM .

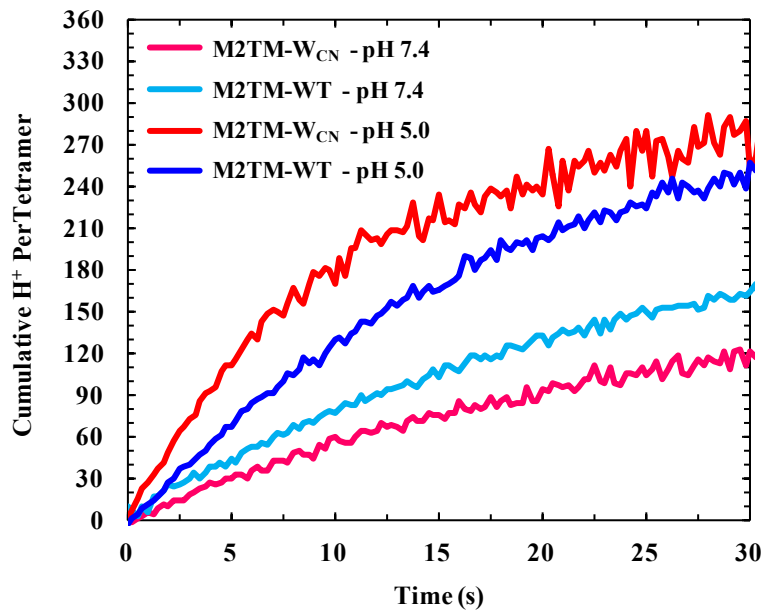


Figure S5: Comparison of the proton fluxes of M2TM-W_{CN} and wild type M2TM, determined from the proteoliposome assay described above. The flux was measured at both pH 7.4 and 5.0, and was accomplished by adjusting the external bulk buffer accordingly while keeping the initial internal liposomal pH constant at pH 7.4. The cumulative proton flux per tetramer was determined to be (1) 6.0 ± 0.5 H⁺/s for the wild-type M2TM and 4.2 ± 0.6 H⁺/s for M2TM-W_{CN} at pH 7.4 and (2) 8.6 ± 0.9 H⁺/s for the wild-type M2TM and 10.6 ± 0.5 H⁺/s for M2TM-W_{CN} at pH 5.0.

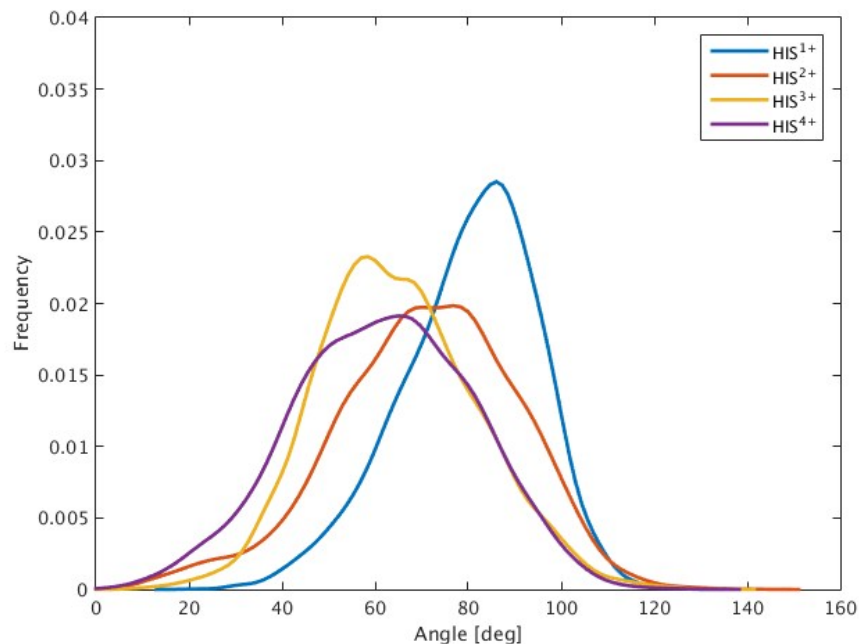


Figure S6: Distribution of the C≡N axis angle with respect to the z-axis of the channel for different His protonation states determined from MD simulations of M2TM-W_{CN}. The corresponding time-averaged C≡N angle ($\theta_{\text{CN-MD}}$) are as follows: His¹⁺: 80.11 ± 14.62 ; His²⁺: 70.91 ± 19.63 ; His³⁺: 64.79 ± 17.12 ; His⁴⁺: 61.80 ± 19.25 .

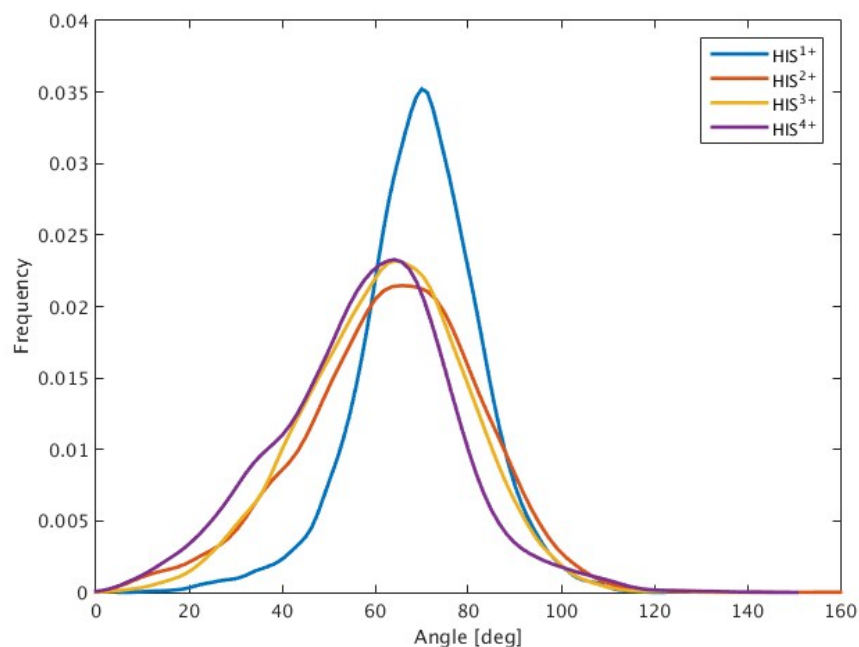


Figure S7: Distribution of the C-H axis angle at C5 position with respect to the z-axis of the channel for the His¹⁺, His²⁺, His³⁺, His⁴⁺ protonation states determined from MD simulations of the wild-type M2TM.⁶

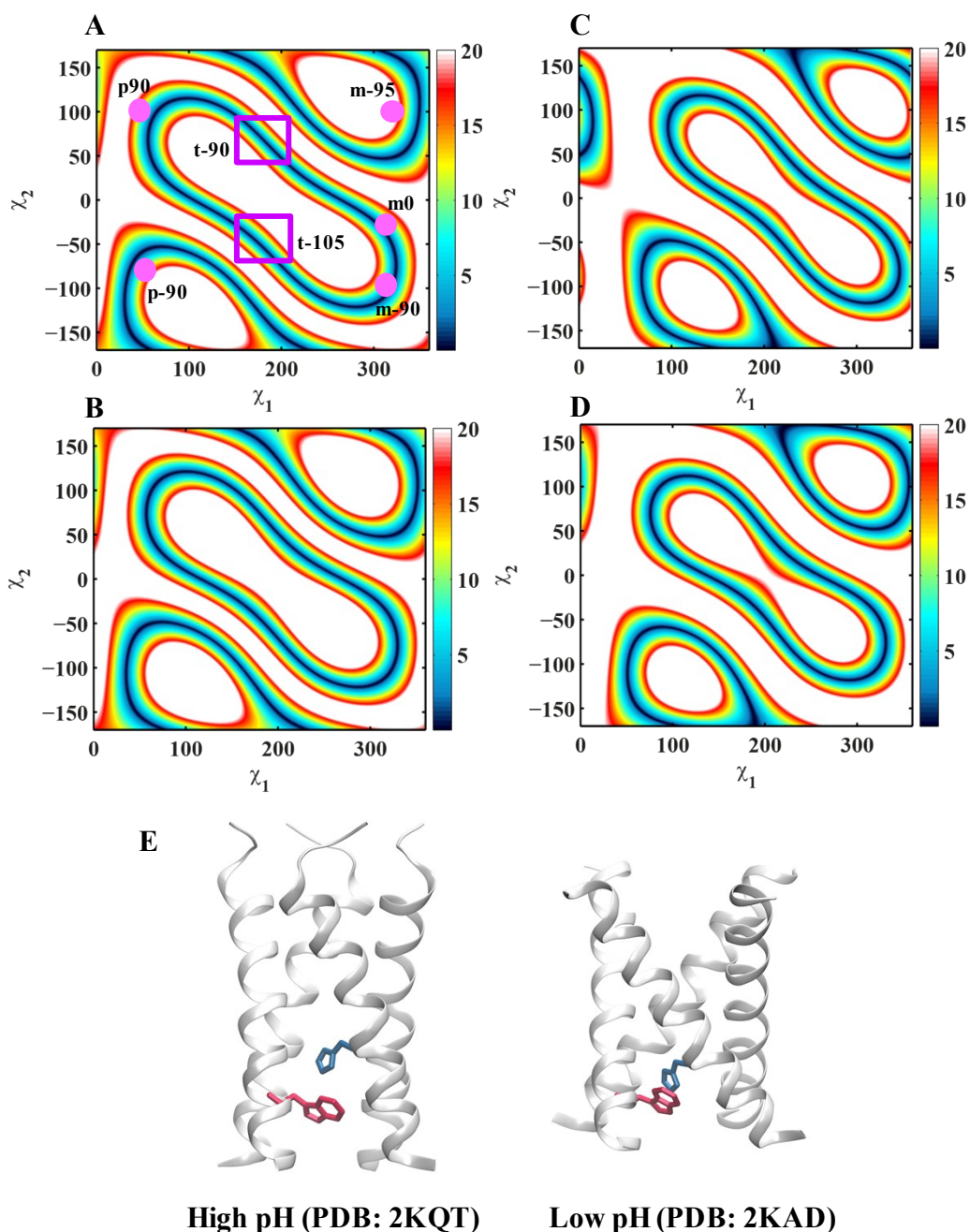


Figure S8: 2D contour plot of the RMSD between the measured and calculated C≡N angles (θ_{CN}) as a function of the torsion angles (χ_1 , χ_2) of Trp41. Four backbone structures, 2QKT (A) and 3LBW (B) for high pH and 2KAD (C) and 3C9J (D) for low pH, were chosen because their helix tilt angles are comparable to those obtained from the ATR-FTIR measurements. The pink circles depicted in (A) represent all the rotameric states of Trp41 that were ruled out based on steric clashes. The purple square represents the two rotameric regimes that were allowed based on the measured θ_{CN} . (E) Trp41 sidechain conformations based on results obtained in Table 2 for high (Right) and low (Left) pH cases.

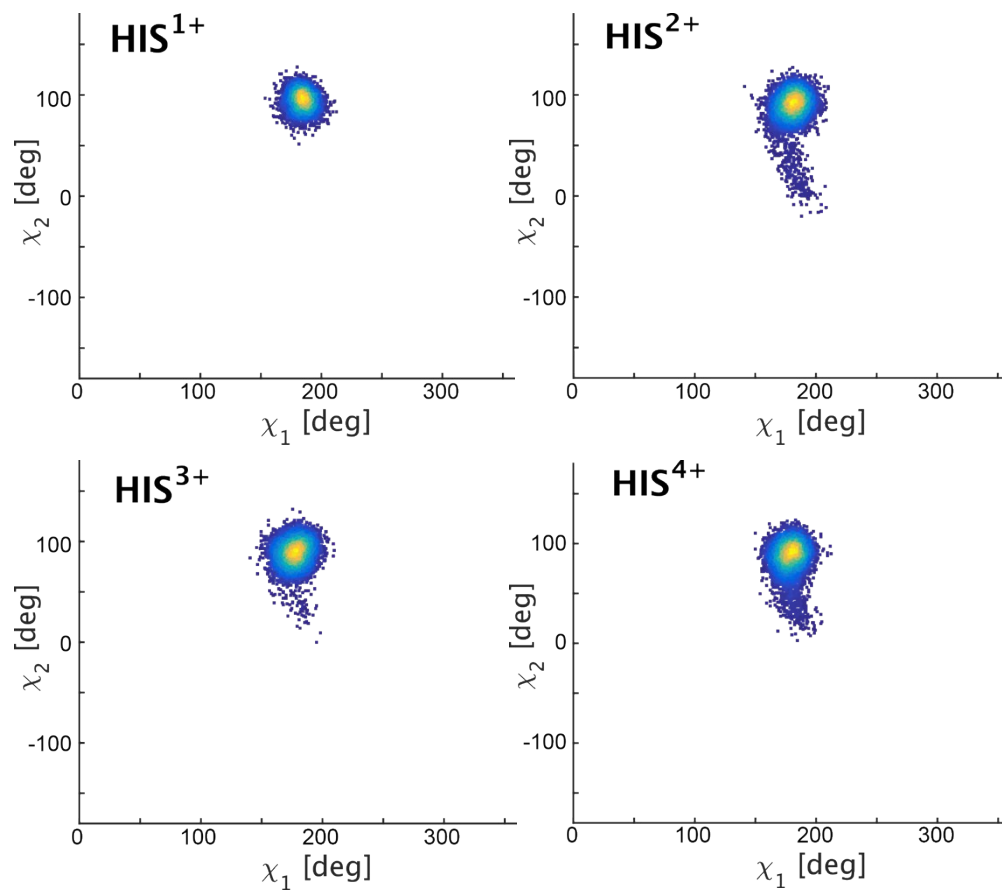


Figure S9: Two-dimensional contour plot of the distribution of torsion angles sampled by Trp_{CN} in the MD simulation. The calculated mean values for χ_1 , χ_2 are as follows: His¹⁺ = 184.55 ± 7.4 , 94.6 ± 9.5 ; His²⁺ = 184.55 ± 7.4 , 94.6 ± 9.5 ; His³⁺ = 177.25 ± 9.2 , 87.89 ± 17.4 ; and His⁴⁺ = 178.95 ± 8.4 , 86.4 ± 16.2 .

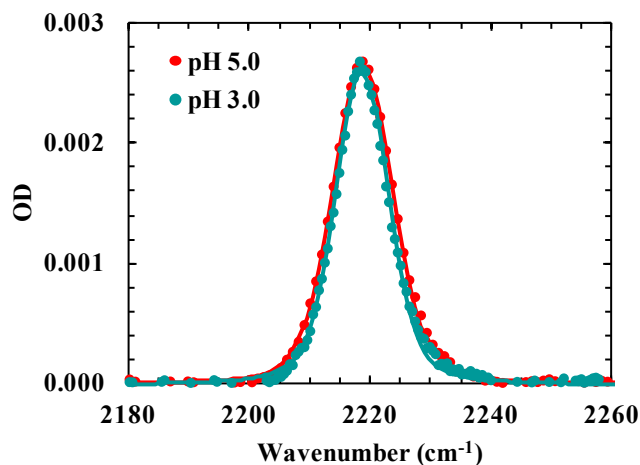


Figure S10: Comparison of the C≡N stretching vibrational bands of M2TM-W_{CN} in the aforementioned lipid bilayers at pH 5.0 and 3.0. These spectra were collected using the ATR-FTIR setup with parallel polarization. The smooth lines are fits to a Voigt profile.

REFERENCES

1. C. Ma, A. L. Polishchuk, Y. Ohigashi, A. L. Stouffer, A. Schön, E. Magavern, X. Jing, J. D. Lear, E. Freire, R. A. Lamb, W. F. DeGrado and L. H. Pinto, *Proc. Natl. Acad. Sci. U. S. A.*, 2009, **106**, 12283-12288.
2. T. Leiding, J. Wang, J. Martinsson, W. F. DeGrado and S. P. Årsköld, *Proc. Natl. Acad. Sci. U. S. A.*, 2010, **107**, 15409-15414.
3. P. Purkayastha, J. W. Klemke, S. Lavender, R. Oyola, B. S. Cooperman and F. Gai, *Biochemistry*, 2005, **44**, 2642-2649.
4. J. K. Williams, Y. Zhang, K. Schmidt-Rohr and M. Hong, *Biophys. J.*, 2013, **104**, 1698-1708.
5. W. Humphrey, A. Dalke and K. Schulten, *J. Mol. Graphics*, 1996, **14**, 33-38.
6. R. Acharya, V. Carnevale, G. Fiorin, B. G. Levine, A. L. Polishchuk, V. Balannik, I. Samish, R. A. Lamb, L. H. Pinto, W. F. DeGrado and M. L. Klein, *Proc. Natl. Acad. Sci. U. S. A.*, 2010, **107**, 15075-15080.
7. J. C. Phillips, R. Braun, W. Wang, J. Gumbart, E. Tajkhorshid, E. Villa, C. Chipot, R. D. Skeel, L. Kalé and K. Schulten, *J. Comp. Chem.*, 2005, **26**, 1781-1802.
8. J. B. Klauda, R. M. Venable, J. A. Freites, J. W. O'Connor, D. J. Tobias, C. Mondragon-Ramirez, I. Vorobyov, A. D. MacKerell and R. W. Pastor, *J. Phys. Chem. B*, 2010, **114**, 7830-7843.
9. W. L. Jorgensen, J. Chandrasekhar, J. D. Madura, R. W. Impey and M. L. Klein, *J. Chem. Phys.*, 1983, **79**, 926-935.
10. A. Brünger, C. L. Brooks and M. Karplus, *Chem. Phys. Lett.*, 1984, **105**, 495-500.
11. S. E. Feller, Y. Zhang, R. W. Pastor and B. R. Brooks, *J. Chem. Phys.*, 1995, **103**, 4613-4621.